Nato ASI Series 'Self-Organization,
Emerging Properties and Learning',
A. Babloyantz, Editor,
(Plenum Press, 199[redacted])

A Model for Synchronous Activity in the Visual Cortex

Christian Kurrer, Benno Nieswand, and Klaus Schulten
Beckman Institute and Department of Physics
The University of Illinois at Urbana-Champaign
405 N. Mathews Ave., Urbana Il 61801, U.S.A.

Key-Words: neural modeling, synchronization, binding-problem, excitable elements, non-linear dynamics.

Abstract

We investigated the problem of figure-ground separation or *binding problem* of image processing in the brain. Recent experiments by Singer et al. have shown in the visual cortex of cat synchronous firing activity among neurons coding similar features. The observations suggest that synchronization may be an important coding principle for information processing in the brain.

The investigations reported here are based on a dynamical description of single neurons as excitable elements with stochastic activity. We demonstrate that sets of weakly coupled neurons of this type can readily develop synchronous activity when subject to coherent excitation. We provide a mathematical analysis of the dynamical model chosen as well aspresent numerical simulations illustrating how synchronous firing can be used in the visual cortex to segment images.

1 Introduction

Most present neural network models, e.g. back-propagation or Hopfield neural nets, use a single state variable to describe a neuron. This state variable represents the firing activity of a physiological neuron. In spite of important

advances using these kind of neural nets, many problems concerning information processing through neural networks are left unsolved. A most important unsolved problem is the socalled *binding problem*[1], which addresses the question how the brain segments images into objects and which neurons correspond to different objects. An example is the figure-ground separation task, i.e. the task to determine the parts of the visual cortex involved in "seeing" the figure and the parts involved in "seeing" the background. This separation is a nontrivial task since both figure and background can contain very similar optical properties such as color, luminosity, texture. Also the figure often does not have a clearly marked outline.

Whereas formerly the *firing rate* of a neuron was assumed to contain all the information transmitted to the brain by sensory neurons, it recently became apparent that in the cortex also the *timing of the firing* of one neuron relative to other neurons in the same cortical area contains essential information. For example, recordings in the olfactory cortex performed by Freeman [2, 3] revealed the occurrence of specific spatio–temporal patterns as soon as a specific odor is identified. However, the problems connected with the measurement of olfactory input seemed to be a major obstacle in establishing quantitative input–output relations between the spatio–temporal patterns and the excitation of the olfactory sensory neurons. Thus it was not easy to discover the mechanisms causing the formation of spatio–temporal patterns and the importance of these for the subsequent steps in information processing.

Important progress in clarifying the role of spatio–temporal patterns in the firing activity of cortical neurons was achieved through recent experiments performed on the visual cortex, initiated by Gray and Singer as well as by Eckhorn et al. [4, 5]. These experiments, for the first time, related the firing correlation of two cortical neurons to the fact that these cortical neurons processed information originating from the same object, such as an illuminated bar shown to the retina. When two neurons processed information originating from the same bar, a situation which can be checked by determining their receptive field beforehand, their firing activity was observed to be synchronized. This result supports the conjecture by von der Malsburg [6] that the "binding" of different stimuli to the same object is achieved through synchronization of the corresponding neural activity in the cortex.

Models for Synchronously Firing Neurons

The new findings on the temporal correlation properties of interacting neurons prompted an investigation of neuron models that incorporate the temporal aspects of the firing of neurons. Some approaches [7, 8, 9, 10] employed oscillator models for a single neuron, and introduced rules that govern the synchronization of these oscillators. These approaches implicitly assume that the normal state of a neuron is described by oscillators which adjust their

phases when subjected to certain kinds of input.

Previous research on coupled nonlinear oscillators [11, 12, 13, 14, 15] elicited essentially three ways of enhancing the synchronization of coupled nonlinear oscillators: (1)increasing *coupling strength* between the oscillators, (2)reducing *spread of the intrinsic frequencies*, and (3) reducing *random pertubations* of the phases of the nonlinear oscillators. Oscillator models for neural networks addressing the synchronization issue, thus, were restricted to stating rules how the excitations of the sensors influences one of these three properties of the population of neurons. With the aid of these rules, some of the experimental results could be reproduced[8, 16].

However, it seems to be hard to translate the rules back into physiological context. This limits the stimulus such models might provide for further experiments, and one may doubt whether the mechanim which are relevant in the brain have actually been described by these rules.

Moreover, periodic oscillations of single isolated neurons have been observed very rarely in experimental recordings. Other models, the ones discussed in [17], employ a more detailed representation of the single neuron incorporating a firing threshold, relaxation and refractory behavior. Their models, however, nevertheless describe single neurons only in a rather abstract fashion.

2 Nonlinear Dynamics Models

To achieve synchronous oscillations in the cortex, our approach employs single neurons which are *excitable element* (EE) [18] rather than oscillators. An EE is a dynamical system with a stable state to which the system relaxes *directly* after *small* perturbations. When the strength of the perturbation exceeds a certain *threshold*, the equilibrium state will only be regained after the system passes through a series of *specific states* which significantly deviate from the stationary state.

In the case of a neuron this corresponds to the phenomenon that small variation of the transmembrane voltage result in a direct relaxation back to the -65 mV resting potential, whereas larger variations cause the cell first to increase its transmembrane potential up to +40 mV before the resting potential is reestablished.

As a mathematical model for such an EE we employ a set of equations known as the Bonhoeffer-van-der-Pol (BvP) or Fitzhugh-Nagumo (FN) equations [19, 20]. These equations, on the one hand, contain only the minimal number of nonlinear terms necessary to yield an EE behavior and, therefore, are mathematically relatively simple; on the other hand, the equations are closely related to the Hodgkin–Huxley description of neurons [21], i.e. to a quantative description of certain neurons (squid giant axon), as shown by Fitzhugh. Hence, the dynamical variables involved can be interpreted in terms of physiological observables.

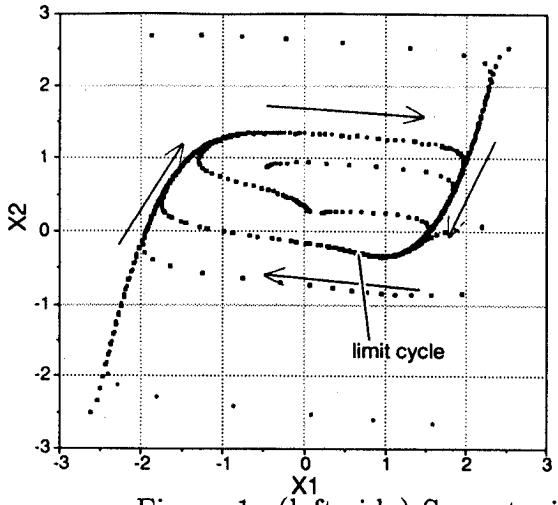

Figure 1: (left side) Some typical phase space trajectories for $z = -0.4$: All trajectories eventually lead into a stable limit cycle. Represented is a stroboscopic view of trajectories for 9 different initial states.

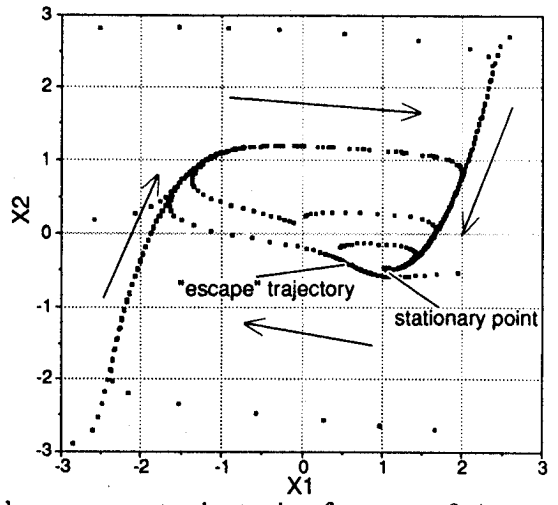

Figure 2: (right side) Some typical phase space trajectories for $z = 0$: All trajectories lead to the stable stationary point at (1.1,-0.5). Note that a trajectory which passes very near by the stationary point will lead the phase point back to its stationary state only after a long path through the phase space.

2.1 The Bonhoeffer-van-der-Pol or Fitzhugh-Nagumo Equations

The dynamics of a neuron in the BvP model is given by the set of equations

$$\begin{aligned} \dot{x_1} &= F_1(x_1, x_2) = c(x_1 - x_1^3/3 + x_2 + z) \\ \dot{x_2} &= F_2(x_1, x_2) = (a - x_1 - bx_2)/c. \end{aligned} \tag{1}$$

According to Fitzhugh's derivation of the BvP equations, x_1 represents the negative transmembrane voltage and x_2 is closely related to the potassium conductivity. The nonlinear term in the first equation reproduces the effect of the voltage-dependent sodium channels. The equations reproduce the response of a single neuron for the choice of control parameters $a = 0.7$, $b = 0.8$, and $c = 3.0$. The dynamical character of the solutions of this system of equations is determined by the parameter z, which corresponds to the excitation current I in the Hodgkin-Huxley equations. Within the physiological range $2.0 > z > -0.6$, the dynamical behavior depends on whether z is larger or smaller than $z_{crit.} \approx -0.34$. For $z > z_{crit.}$ the variables (x_1, x_2) asymptotically reach a stable fixed point, whereas for $z < z_{crit.}$ the solutions are periodic in time. The latter solution corresponds to a periodic firing of neurons. The phase portrait for these two dynamical modes is shown in Figs. 1 and 2.

Whereas the BvP model describes a neuron which at z_{cr} abruptly changes its behaviour from complete silence to firing at a fairly constant frequency, Treutlein and Schulten [22] showed that the model can be made more realistic by adding noise, which opens the possibility of varying the firing frequency

smoothly from zero to its maximal value. The resulting dynamics of the neuron is described by

$$\begin{aligned} \dot{x_1} &= F_1(x_1, x_2) + \eta_1(t) &&= c(x_1 - x_1^3/3 + x_2 + z) + \eta_1(t) \\ \dot{x_2} &= F_2(x_1, x_2) + \eta_2(t) &&= (a - x_1 - bx_2)/c + \eta_2(t) \end{aligned} \tag{2}$$

where $\eta_i(t), (i = 1, 2)$ represents Gaussian white noise with amplitude $\sigma = \sqrt{2\beta^{-1}}$ charactarized through the relations

$$\langle \eta_i(t) \rangle = 0, \qquad \langle \eta_i(t_1)\eta_j(t_2) \rangle = \beta^{-1}\, \delta(t_1 - t_2)\, \delta_{ij} \ . \tag{3}$$

These equations were investigated for the range of z leading to limit cycle dynamics in [23]. Here, we will focus on a range of z where these equations describe an EE (corresponding to the case shown in Fig. 2). Because of the noise added to the BvP dynamics, the phase point will not be trapped at the stationary state, but rather exhibits diffusion-like behavior in the phase space. Eventually it will reach an *escape trajectory*, shown in Fig. 2, which attracts the phase point to negative x_1 values, and in this way action potentials are generated. The influence of the noise thus leads to trajectories that follow a *stochastic limit cycle.*

The rate by which a *stochastic excitable element* (SEE) releases action potentials depends on the amplitude of the noise as well as on the distance between the stationary point and the closest escape trajectory. This distance determines the excitability of the EE and depends on the parameter z. A change in z will thus influence the average firing rate of the SEE, as shown in Fig. 3.

A change in the excitation parameter z is thus the key physiological mechanism by which the behavior of an individual neuron is controlled in our model. In the remaining part of this text, we will investigate how this parameter influences the synchronicity of firing of coupled neurons, and how this firing synchronicity can serve visual information processing.

3 Dynamics of Coupled Neurons

To describe the dynamics of coupled neurons, we expanded the BvP-equations to include an interaction term between neurons

$$\begin{aligned} \dot{x_{1,i}} &= c(x_{1,i} - x_{1,i}^3/3 + x_{2,i} + z) + \eta_1(t) + \textstyle\sum_j W_{j\to i}(t) \\ \dot{x_{2,i}} &= (a - x_{1,i} - bx_{2,i})/c + \eta_2(t). \end{aligned} \tag{4}$$

The coupling of neuron j to neuron i is described by

$$W_{j\to i}(t) = \theta(-x_{1,j}(t)) \cdot (x_{1,j}(t) - x_{1,i}(t)) \cdot w_{ji}, \quad i,j \in \{1, 2, \ldots N\}. \tag{5}$$

This interaction term is to be interpreted as follows : (1) neuron j only excites neuron i when neuron j is momentarily firing, i.e when the step function θ is 1; (2) the interaction strength is proportional to the difference in the voltages of the neurons, i.e. an excited cell cannot be further excited effectively by another excited cell; (3) the interaction strength is scaled by "synaptic weights" w_{ji}.

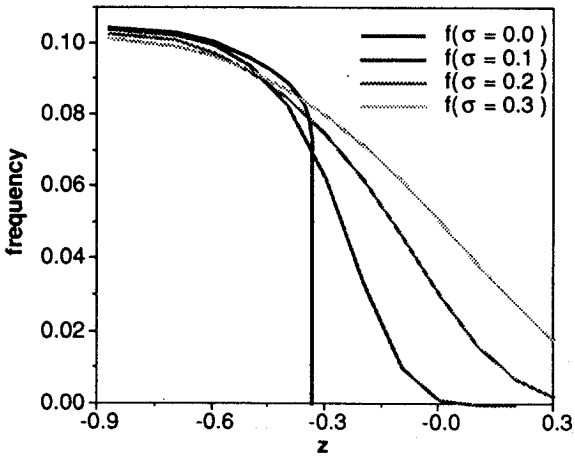

Figure 3: Dependence of the average frequency of action potentials on the input parameter z in the BvP–model (Eq. 2) for different noise amplitudes σ. The frequencies were obtained by integrating the stochastic equations (Eq. 2) over a long time and counting the number of action potentials released.

A Measure for Synchronicity

In the following we provide a measure for the time correlation of the firing activity of populations of coupled neurons. In case individual neurons are described by nonlinear oscillators, the synchronicity of N oscillators can be determined in terms of the phases $\phi_i(t)$ of the individual oscillators as follows:

$$C_{lc}(t) = \frac{1}{N(N-1)} \sum_{i \neq j}^{N} cos(\phi_j(t) - \phi_i(t)). \tag{6}$$

The definition of a phase $\phi_i(t)$ of the individual oscillators can be expanded to stochastic nonlinear oscillators in close proximity to the limit cycle [11]. In general, however, it is not easy to find a meaningful definition of the phase of an SEE. Since each SEE will stay an undetermined amount of time in the vicinity of the stationary point, the knowledge that two systems are close to each other on the stochastic limit cycle does not allow a prediction of the time when these two systems will start their next turn on the stochastic limit cycle. Therefore, the relative location of SEE's in the phase space is not a good basis for defining their synchronicity. For this reason we define the synchronicity of coupled SEE in terms of the function $t_i(t)$ for neuron i; this function gives at the instant t the time t_i at which neuron i started to fire last, the beginning of firing being defined as the time when x_1 crosses the x_2-axis from $x_1 > 0$ to $x_1 < 0$. The synchronicity C_{SEE} for SEE's was then defined accordingly as

$$C_{SEE}(t) = \frac{1}{N(N-1)} \sum_{i \neq j}^{N} cos(2\pi \frac{(t_j(t) - t_i(t))}{T}). \tag{7}$$

where T is the average firing frequency of the population of SEEs. This definition becomes equivalent to the definition in Eq. (6) when z is changed from $z > -0.34$ to $z < -0.34$, i.e. when the SEE's adopt a limit cycle which does not require noise, as shown in Fig. 1.

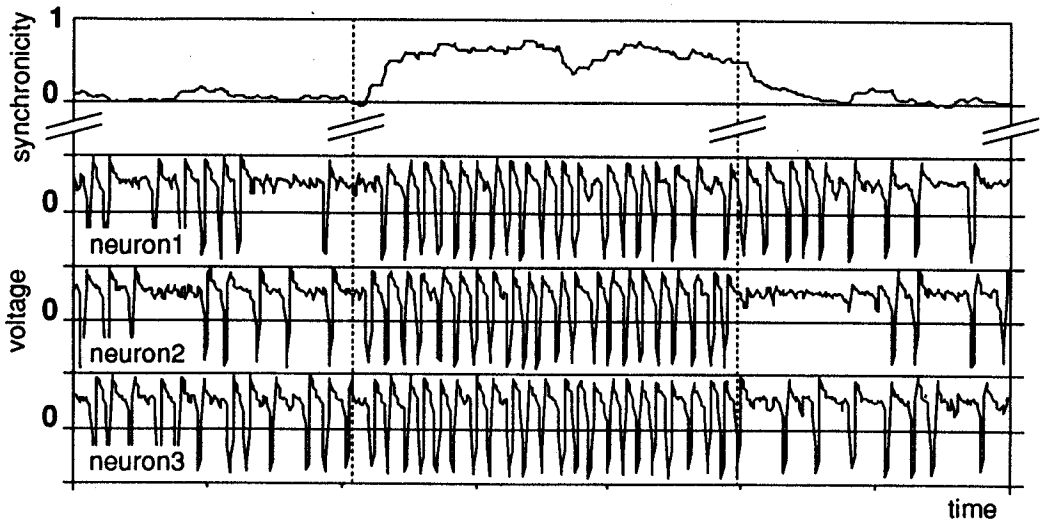

Figure 4: Simulation of the firing activity of 50 coupled BvP neurons. At the time indicated by the vertical dashed lines, the excitation z is first increased from $z = -0.16$ to $z = -0.24$ and then restored to the initial value $z = -0.16$. The top trace shows the correlation function $C_{SEE}(t)$. The synchronicity C_{SEE} responds to the change in z with a delay of about two firing cycles. The lower three traces represent the transmembrane voltage signal $x_1(t)$ of three neurons. (noise amplitude is $\sigma = 0.1$, synaptic weights are all $w_{i,j} = 0.01$).

3.1 Dynamical Properties of Coupled SEEs

To study the dynamics of a population of coupled SEE's, we numerically integrated the dynamics of 50 uniformly coupled SEE's described by Eqs. (4).

Figure 4 shows the result of a typical simulation. In the initial time interval the neurons were only slightly excited ($z = -0.16$). At the instant indicated by the first dashed line, the excitation value is suddenly increased ($z = -0.24$) for a time period lasting to the instant indicated by the second dashed line, at which time the value of $z = -0.16$ is restored. The uppermost graph shows how the correlation function C_{SEE} defined in Eq. 7 responds to the changes of z. One can see, that the correlation function responds within approximately two periods to changes of z. This fast synchronization and desynchronization is a key feature of our model and is in good agreement with experimental data [4]. The three lower traces in Fig. 4 show the voltage signal $x_1(t)$ of three of the 50 neurons. At low excitation values ($z = -0.16$), the neurons fire at a relatively low frequency. As the excitation of the neurons increase ($z = -0.24$), the firing frequency rises and at the same time, the firing pattern of the coupled neurons becomes synchronized.

In Fig. 5 we present histograms showing the time correlation of action potentials for large populations of neurons for different values of the excitation parameter z. The histograms show the firing probability of neuron i at a time δt after neuron j has fired. For the first two simulations with $z = -0.12$ and $z = -0.16$ the firing is essentially asynchronous. There is only a small

correlation due to the finite size of the neuronal population ($N = 100$). For $z = -0.20$ and $z = -0.24$ the firing is synchronous. The synchronicity becomes more pronounced as the parameter z is further lowered below the value of $z_{crit} \approx -0.185$, for which the system would show a synchronization phase transition with order parameter C_{SEE} in the limit of $N \to \infty$. (A detailed discussion of this phase transition will be published elsewhere.)

Figure 6 shows the the firing frequencies of coupled and uncoupled neurons and order parameter C_{SEE} as a function of z, obtained from simulations of $N = 500$ neurons. It is worth noting that this transition in the firing pattern already occurs at quite low excitation values, much lower than necessary for an individual neuron to become continuously firing.

Experiments by Gross and Kowalsky [24] have shown that the synchronous firing activity in populations of randomly coupled neurons is usually connected with intense firing activity. This relation is naturally reproduced by our model (see Fig. 6).

4 Artificial Cortical Geometry

We simulated the dynamics of the neural activity in a system where the coupling strengths between any two neurons are no longer uniform, but mimic the coupling scheme of neurons in the visual cortex. The aim was to re-

Figure 5: Histograms showing the time correlation of firing of 100 homogeneously coupled neurons. Plotted are the number of times that two firing events have been recorded with a time difference of δt in a simulation involving 100 neurons. The values of z are -0.12 for (A), -0.16 for (B), -0.20 for (C), and -0.24 for (D). The time span over which firing events are correlated increases with lowered z-value (noise amplitude is $\sigma = 0.1$, synaptic weights are all $w_{i,j} = .005$).

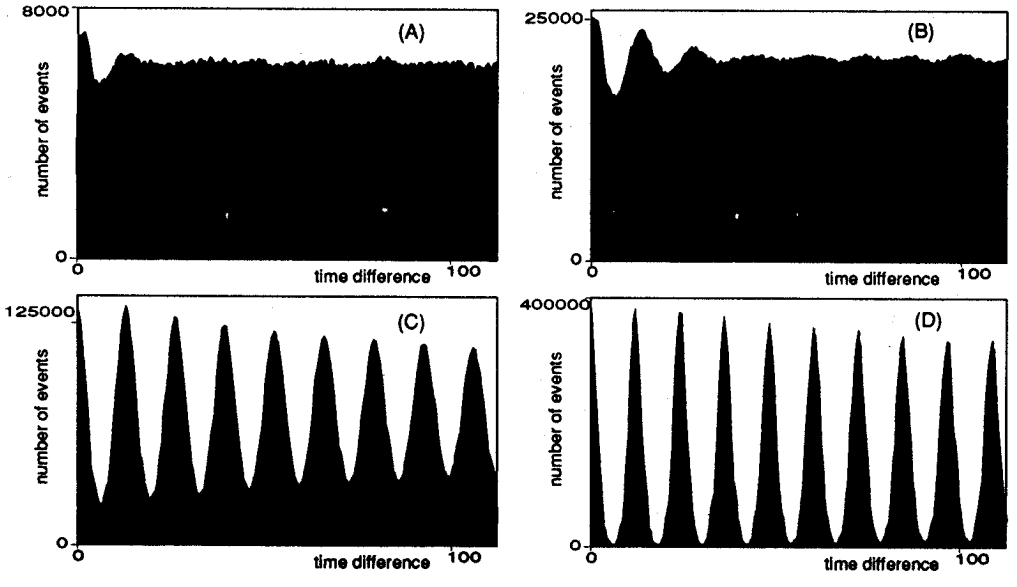

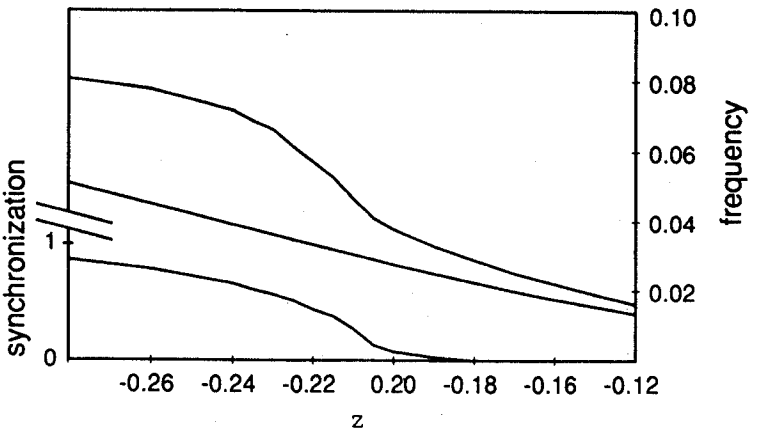

Figure 6: Correlation and firing frequency as a function of the excitation parameter z. The graph shows the dependence on z of the frequency of coupled neurons (upper graph) compared to the frequency of uncoupled neurons (middle graph). The bottommost graph gives the corresponding C_{SEE} for the coupled system which is simulated using 500 neurons coupled by $w_{i,j} = 0.001$ and with noise $\sigma = 0.1$.

produce experiments by Gray and Singer [4] in which oriented light bars presented to the retina of a cat evoked synchronous activity in area 17 of the visual cortex.

Extensive neuroanatomical studies based on Hubel and Wiesel's pioneering works [25, 26] have resulted in information on the structure of the visuocortical pathways: activity in the retina projects onto the visual cortex in such a way, that signals from nearby areas on the retina project to nearby areas of the visual cortex. On a lower hierarchal level one finds cells that respond best to stimuli of a specific orientation. Cells representing all orientation prefences are grouped in the socalled hypercolumns of the primary visual cortex.

Accordingly, we distribute the neurons in our simulation on a two dimensional grid labeling them by their horizontal and vertical position (i, j) and assigning them four different orientation preferences $\theta_{i,j} = 0°, 45°, 90°, 135°$ relative to the x-axis according to the scheme displayed in Figure 7. This distribution scheme ensures that four neurons on any 2×2 area of the artificial cortex assume all four orientation preferences. The scheme is a caricature of the observed orientation homogeneity in the hypercolumns of the cortex [27, 28].

The coupling between two neurons (i, j) and (i', j') was described as in Eq. 5. The weights $w_{i,j}$ are chosen

$$w_{i,j;i',j'} = w\max \cdot w^{(1)}_{i,j;i',j'} \cdot w^{(2)}_{i,j;i',j'} \cdot w^{(3)}_{i,j;i',j'} \tag{8}$$

where

$$w^{(1)}_{i,j;i',j'} = \cos^2(\theta_{i,j} - \theta_{i',j'}) \tag{9}$$

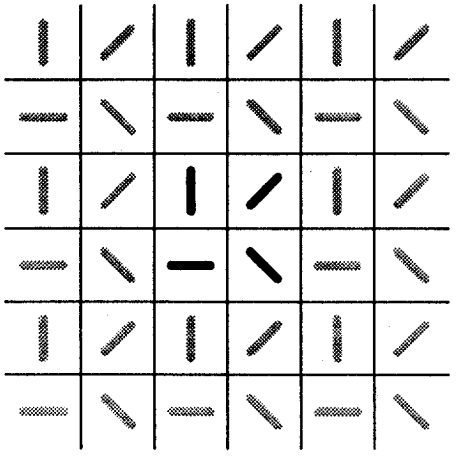

Figure 7: Distribution of orientation preferences of neurons in the artificial cortex. The center part of the figure shows a quadruple of neurons which represent an orientation column.

$$w^{(2)}_{i,j;i',j'} = \exp\left(-\frac{\sqrt{(i-i')^2-(j-j')^2}}{r_0}\right) \tag{10}$$

$$w^{(3)}_{i,j;i',j'} = \frac{\cos^2(\frac{\theta_{i,j}+\theta_{i',j'}}{2}-\xi_{i,j;i',j'})+1}{2}. \tag{11}$$

and $\xi_{i,j;i',j'}$ is the orientation of the connection vector between neurons (i,j) and (i',j'). The weights are scaled by the global parameter $w_{\max}$. The three factors in this formula describe how the coupling strength depends (1) on the relative orientation preference, (2) on the distance, and (3) on the alignment of the orientation preferences of neighboring neurons, respectively.

Rotating Bar on the Artificial Cortex

We use our artificial cortex to simulate the synchronous activity evoked in the visual cortex by a rotating bar presented to the retina. This bar is shown schematically in Fig. 8. In these simulations, cortical neurons the receptive fields of which overlap with the light bar receive an additional excitation of strength Δz

$$\begin{aligned} \dot{x_{1,i}} &= c(x_{1,i} - x_{1,i}^3/3 + x_{2,i} + (z+\Delta z_{i,j}) + \eta + \textstyle\sum_j W_{j\to i} \\ \dot{x_{2,i}} &= (a - x_{1,i} - bx_{2,i})/c + \eta(t), \end{aligned} \tag{12}$$

where

$$\Delta z = \begin{cases} \Delta z_{\max}\cdot\cos^2(\theta_{i,j}-\theta_0) & : \text{for neurons receiving input} \\ & \quad \text{from the light bar} \\ 0 & : \text{for all other neurons} \end{cases} \tag{13}$$

with θ_0 being the orientation of the bar. The other parameters are $z=-0.16$, $\Delta z_{\max}=-0.16$, $\sigma=0.1$, and $w_{\max}=0.04$.

We simulated a light bar presented through the retina to an array of 25×25 neurons. The light bar initially covered the central portion of the

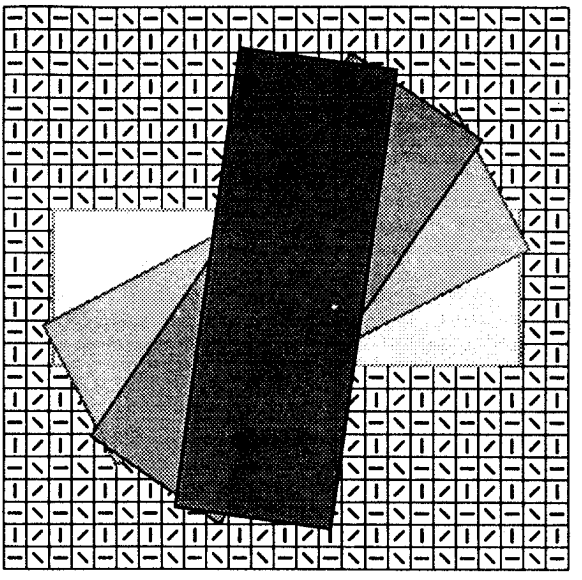

Figure 8: Scheme showing the geometry of a rotating light bar, providing excitation to the receptive fields of 25×25 neurons.

retina which is connected to 7×21 neurons of the cortex then rotated around its center with a constant angular velocity (see Fig. 8). In these simulations, the neurons covered by the light bar and having an orientation preference approximately parallel to the bar engaged in synchronous, periodic oscillation. Neurons covered by the light bar, but having an orientation preference approximately perpendicular to the orientation of the bar, did not fire periodically and had a much lower frequency; their firing spikes however were correlated with the firing spikes of the neurons with correct orientation preference. Figure 9 presents a histogram of time differences between spikes for the two populations of neurons, those covered by the bar (1) and those not covered by the bar (2). One can see that firing correlation is maintained over a long time for population (1). The population (2) does not show long time correlation; the small wiggle in the correlogram is caused by the influence of the neurons of (1), which s excite adjacent neurons of population (2) .

As the bar rotates, the population (1) of excited neurons constantly changed due to the rotation of the bar, with new neurons added and other neurons leaving the population. The ability of these neurons to respond quickly with their firing activity, i.e. quickly synchronize or desynchronize with the rest of the population, was thereby important for the coding of the location of the bar in terms of synchronous firing activity. Although different neurons participated in the synchronous activity during the rotation of the bar, the phase of the oscillations was preserved over a time period of a full turn of the object.

5 Conclusion

Our investigations demonstrated that synchronous periodic oscillations appear in populations of SEE's with sufficiently large external excitation z. Both synchronization and desynchronization occur within few firing periods after modification of z. We believe that this behaviour is relevant to under-

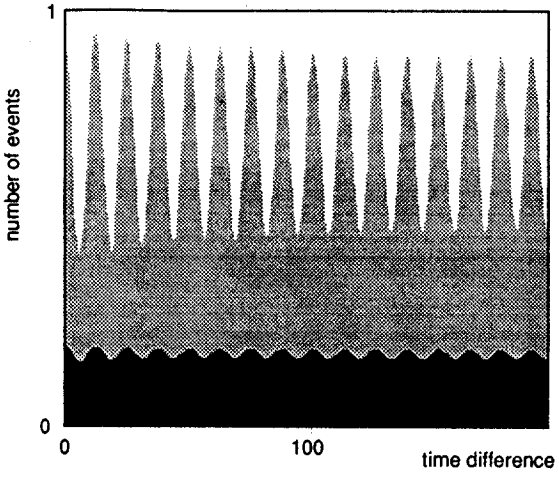

Figure 9: Histograms showing the firing time correlation of different populations of the cortical neurons. Plotted are the number of times that two firing events of neurons of the same population have been recorded with a time difference of δt. The upper curve shows the counts for neurons (1) covered by the bar, the lower curve shows the counts for neurons (2) not covered by the bar. Neurons (1) under the bar fire at a higher frequency and with larger correlation. ($z = -0.16$, $\Delta z_{\max} = -0.16$, $\sigma = 0.1$, and $w_{\max}$=0.04).

stand the occurrence of synchronous firing in physiological neural networks as observed in [4, 5].

The only way to achieve synchronization and desynchronization in oscillator models, rather than SEE models, is to shift the phases of single oscillators. This shift is driven by the competition of two mechanisms, coupling and noise. This shift develops only slowly, unless coupling and noise are changed drastically. SEE models show a different, and more suitable behaviour. Synchronicity is controlled by the excitability of the neurons. Periodic activity only arises as the excitability of the neurons is increased beyond a critical threshold z_{crit}. The single neurons themselves have no autonomous phase, but respond with their firing activity such that periodic activity emerges very rapidly in a population of coupled SEEs. While oscillator models have been similarly successful in describing the state of collective oscillations in neural networks, the SEE model also describes well the state of non-synchronous firing. Furthermore the model reproduces the relation between high firing frequency and synchronicity experimentally measured for randomly connected networks [24].

The model in based on a description of single neurons in terms of observable dynamic variables. The results presented demonstrate a simple mechanisms by which synchronization can be induced and exploited for solution of the binding problem.

Acknowledgement The authors wish to thank Thomas Martinetz, Klaus Obermayer, Helge Ritter and Guenter W. Gross for useful discussion. This work has been supported by the University of Illinois at Urbana-

Champaign, by a grant of the National Science Foundation DMR 89-20538 (through the Materials Research Lab of the University of Illinois), and by a grant of the National Science Foundation DIR 90-15561.

References

[1] J. E. Hummel and I. Biederman. Dynamic binding: A basis for the representation of shape by neural networks. Manuscript submited to the 12th Annual Meeting of the Cognitive Science Society, Cambridge, MA, July 1990.

[2] W. J. Freeman. *Mass Action in the Nervous System.* Academic Press, New York, 1975.

[3] C. S. Skarda and W. J. Freeman. How brains make chaos in order to make sense of the world. *Behavioural and Brain Sciences*, 10:161–195, 1987.

[4] C. M. Gray and W. Singer. Stimulus-specific neuronal oscillations in orientation columns of cat visual cortex. *PNAS*, 86:1698–1702, 1989.

[5] R. Eckhorn, R. Bauer, W. Jordan, M. Brosch, W. Kruse, M.Munk, and H. J. Reitboeck. Coherent oscillations: A mechanism of feature linking in the visual cortex? multiple electrode and correlation analysis in the cat. *Biol. Cybernetics*, 60:121–130, 1989.

[6] C. von der Malsburg. The correlation theory of brain function. Internal Report 81-2, Department of Neurobiology, Max Planck Institute for Biophysical Chemistry, Göttingen, FRG, 1981.

[7] R. Eckhorn, H. J. Reitboeck, M. Arndt, and P. Dicke. A neural network of feature linking via synchronous activity. In *Models of Brain Function.* Cambridge University Press, 1989.

[8] H. Sompolinsky, D. Golomb, and D. Kleinfeld. Global processing of visual stimuli in a neural network of coupled oscillators. *PNAS*, 87:7200–7204, 1990.

[9] H. G. Schuster and P. Wagner. A model for neuronal oscillations in the visual cortex. In *Parallel Processing in Neural Systems and Computer*, pages 143–146. North Holland, 3 1990.

[10] T. B. Schillen and P. König. Coherency detection by coupled oscillatory responses - synchronizing connections in neural oscillator layers. In *Parallel Processing in Neural Systems and Computer*, pages 139–142. North Holland, 3 1990.

[11] A. T. Winfree. *The Geometry of Time.* Springer-Verlag, Berlin Heidelberg New York, 1980.

[12] Y. Kuramoto. *Chemical Oscillations, Waves, and Turbulence.* Springer Verlag, New York, 1984.

[13] Y. Kuramoto and I. Nishikawa. Statistical macrodynamics of large dynamical systems. case of a phase transition in oscillator communities. *J. Stat. Phys.*, 49(3/4):569, 1987.

[14] L. L. Bonilla, J. M. Casado, and M. Morillo. Self-synchronization of populations of nonlinear oscillators in the thermodynamic limit. *J. Stat. Phys.*, 48(3/4):571, 1987.

[15] S. H. Strogatz and R. E. Mirollo. Collective synchronization in lattices of nonlinear oscillators with randomness. *J. Phys. A*, 21:L699–L705, 1988.

[16] D. M. Kammen, P. J. Holmes, and C. Koch. Personal communications.

[17] H. J. Reitboeck, R. Eckhorn, M. Arndt, and P. Dicke. A model for feature linking via correlated neural activity. In *Synergetics of Cognition.* Springer Verlag, 1989.

[18] A. V. Holden, M. Markus, and H. G. Othmer, editors. *Nonlinear Wave Processes in Excitable Media.* Plenum Press, London, 1990.

[19] R. Fitzhugh. Impulses and physiological states in theoretical models of nerve membranes. *BJ*, 1:445, 1961.

[20] J. Nagumo, S. Arimoto, and S. Yoshizawa. An active pulse transmission line simulating nerve axon. *Proceedings of the IRE*, 50:2061–2070, 1962.

[21] A. L. Hodgkin and A. F. Huxley. A quantitative description of membrane cuurent and its application to conduction and excitation in nerve. *J. Physiol. London*, 117:500, 1952.

[22] H. Treutlein and K. Schulten. Noise-induced neural impulses. *Eur. Biophys. J.*, 13:355–365, 1986.

[23] Ch. Kurrer and K. Schulten. Effect of noise and perturbations on limit cycle systems. *Physica D*, 1990. in press.

[24] G. W. Gross and J. M. Kowalski. Experiments and theoretical analysis of random nerve cell network dynamics. In *Neural Networks: Concepts, Applications, and Implementations.* Prentice Hall, 1990. in press.

[25] D. H. Hubel and T. N. Wiesel. Receptive fields, binocular interaction and functional architecture in the cat's visual cortex. *J. Physiol.*, 160:106–154, 1962.

[26] D. H. Hubel and T. N. Wiesel. Sequence regularity and geometry of orientation columns in the monkey striate cortex. *J. Comp. Neurol.*, 158:267–294, 1974.

[27] G. Blasdel and Salama. Voltage sensitive dyes reveal a modular organisation in monkey striate cortex. *Nature*, 321:579, 1986.

[28] K. Obermayer. A principle for the formation of the spatial structure of cortical feature maps. *Proc. Natl. Acad. Sci., USA*, in press, 1990.